UNITED NATIONS UNIVERSITY
UNU-GTP
Geothermal Training Programme

Orkustofnun, Grensasvegur 9,
IS-108 Reykjavik, Iceland

Reports 2015
Number 19

USE OF GEOTHERMAL ENERGY FOR SEAWATER DESALINATION IN THE GALÁPAGOS ISLANDS, ECUADOR

Andrés Lloret C.
National Institute of Energy Efficiency and Renewable Energy, INER
Av. 6 de Diciembe N33-32 e Ignacion Bossano
ECUADOR
andres.lloret@iner.gob.ec, andreslloret@gmail.com

ABSTRACT

The lack of reliable sources of potable water is a health and social problem in the Galápagos. The presence of geothermal resources in the islands opens a window of opportunity for the development of a geothermal energy-driven desalination system. Analysis on the available research studies on three shield volcanoes located on the western side of Isabela Island, reveals that Alcedo Volcano presents the most active hydrothermal system with a liquid-dominated reservoir. This type of system is suitable to achieve the separation of nearly salt-free fresh water by implementing a Single Stage Flash Geothermal desalination system (SSF-G). The concept implies the use of geothermal brine from a separator unit as the heat input source for desalination, while producing electricity from the steam to power the plant totally detached from the grid. Results from a thermodynamic model and exergy analysis of the system, using Engineering Equation Solver (EES) software, show that the geothermal resource can be successfully coupled to this desalination method. It also reveals that most of the energy received from the well, exits the plant while still containing substantial exergy, which can be used to perform usable work by the system. As a result of irreversibilities, exergy destruction occurs in all the heat exchangers of the desalination process. As the area under study is within a National Park, the impacts of the plant need to be considered especially. An accounting framework that measures social, environmental and financial performance in terms of sustainability was undertaken in this study. It indicates that an improvement in water quality on Isabela Island, using geothermal energy, would have significant positive impacts on these dimensions of performance. Detailed geophysical studies using AC resistivity methods, and an exploratory drilling campaign is needed to achieve more conclusive information about the feasibility of this project. The results, collected from these studies will help obtaining more information regarding the cap rock, host rock, and hydrothermal alteration of the geothermal prospects located in the Island.

1. INTRODUCTION

The Galápagos Islands, located 973 km off the west coast of Ecuador, are known by its unique biodiversity which inspired Charles Darwin´s theory of evolution. They are also considered to be one of the most volcanically active regions on earth. With 25,124 inhabitants (INEC, 2015), the population in the Galápagos is spread out in small towns across 4 of the 18 islands.

Presently, the lack of provision and access to a reliable source of potable water is a health and social problem for the community due to very limited sources of fresh water. Bacteriological contamination of the municipal tap water system (López et al., 2007), along with high concentrations of dissolved salt, force islanders to continuously turn to unregulated private alternatives for fresh water supply (Walsh et al., 2010). Moreover, embedded use of fossil fuels, waste generation and the depletion of existing aquifers, resulting from the current local water supply model, compromises its sustainability when faced with an uncontrolled population increase.

Advances in water desalination technologies have made production of potable water a viable option over the last few years. In 2007, the world´s desalinated water production was 40 million m^3/day (Khawaji et al., 2008). Over the following 7 years it doubled, reaching 81 million m^3/day in 2014 (Ghaffour et al., 2015). According to the Global Water Intelligence (Olsson, 2015), the total global desalination capacity is expected to reach over 100 million m^3/day by the end of 2015.

Water desalination by means of renewable energy has been proven to be technically and economically feasible in remote, isolated, or water scarce locations. Renewable sources such as solar, geothermal and wind have already been researched and tested to work as the main energy input for desalination. Goonsen et al. (2014) provide an overview of pilot Renewable Energy (RE) driven desalinations systems installed around the world.

In this study, the potential use of geothermal energy for seawater desalination in Isabela Island is analysed. A review is done on the existing geothermal activity documented by Geist et al. (1994), Goff et al. (2000), and Naumann et al. (2002), to identify a potential geothermal prospect for the application of a geothermal energy-driven desalination system on the island. A thermodynamic model and exergy analysis of a proposed Single Stage Flash geothermal desalination system (SSF-G) is done using Engineering Equation Solver (EES) software. The model will simulate the distillation of nearly 276 m^3 of seawater per day, using geothermal brine from a separator unit as the heat input source for the desalination process. The inflow of potable water from this process will be sufficient to match the average consumption of water per day in the island (Guyot-Téphany and Liu, 2011). The design will also simulate the use of high enthalpy geothermal steam to produce electricity for a stand-alone operation, enabling the desalination plant to run in an off-grid mode. The study concludes with a simplified Triple Bottom Line (TBL) assessment approach to discuss the economic, social and environmental aspects of a potential geothermal desalination project.

2. JUSTIFICATION

2.1 Overview of the problem

The Province of Galápagos, with a total population of 25,124 is divided into three cantons: Isabela (9%), Santa Cruz (60%) and, San Cristobal (31%) (Figure 1).

Over the last 40 years, the majority of inhabitants from the islands have been supplied brackish water from the municipal service. It is presently the only subsurface source available; it is extracted from basal aquifers and distributed by local municipalities to its citizens. Figure 2 shows the main sources of water on Isabela Island. The resource is composed of rain water from the highlands, and three main aquifers: El Chapin, el Manzanillo, and San Vicente. However, these aquifers cannot sustainan an uncontrolled urbanization growth, which leads to an increase in demand. As a result, water supply restrictions are presently in place, although so far they have not been proven effective and, in some cases, have created other water related issues (Guyot-Téphany et al., 2012). In addition, improvised (and unregulated) private desalination business and, imported bottled water from the mainland, provide the daily supply of freshwater required to sustain domestic and commercial activities in the island.

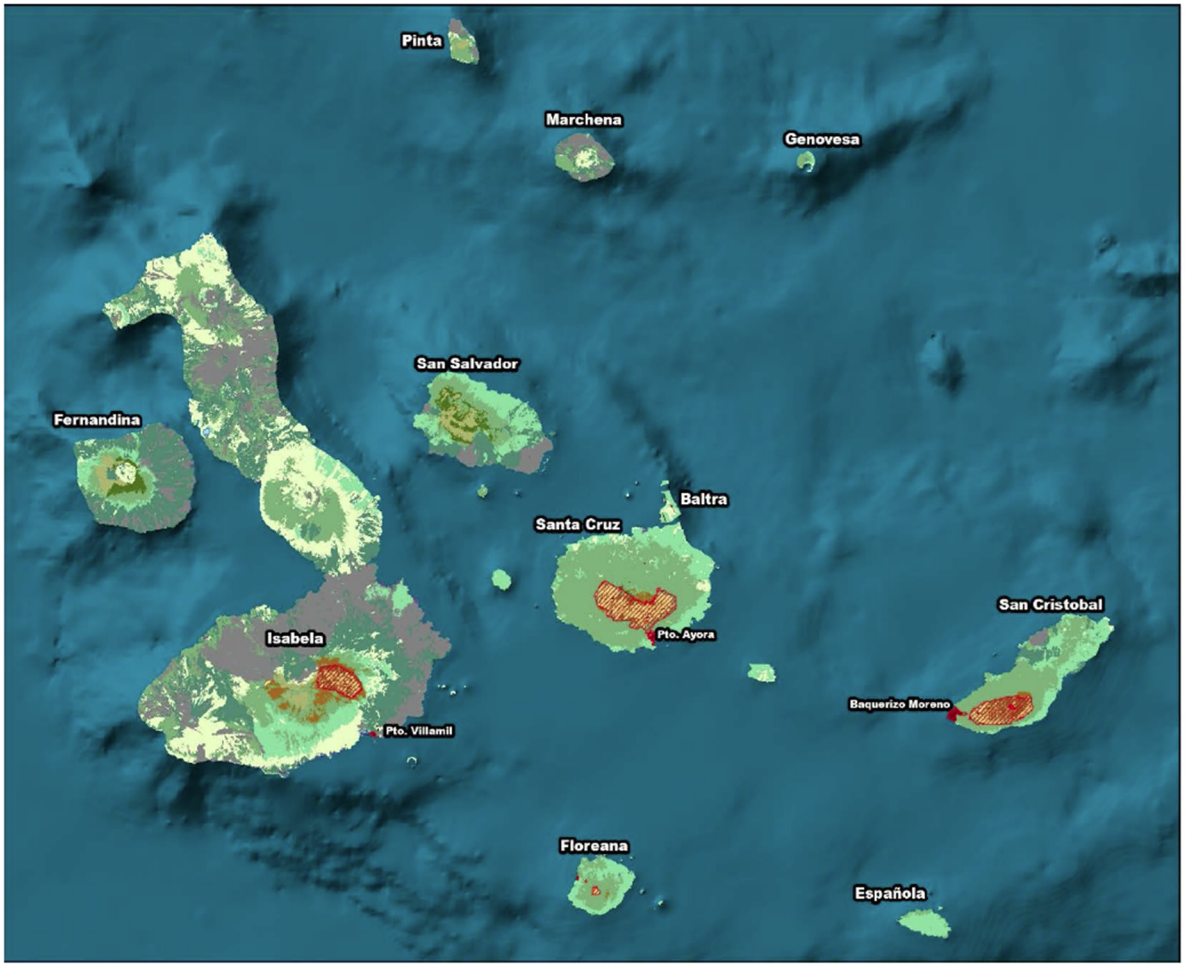

FIGURE 1: Demographic map of the Galápagos Islands
(CEPROEC-IAEN and SENPLADES, 2014)

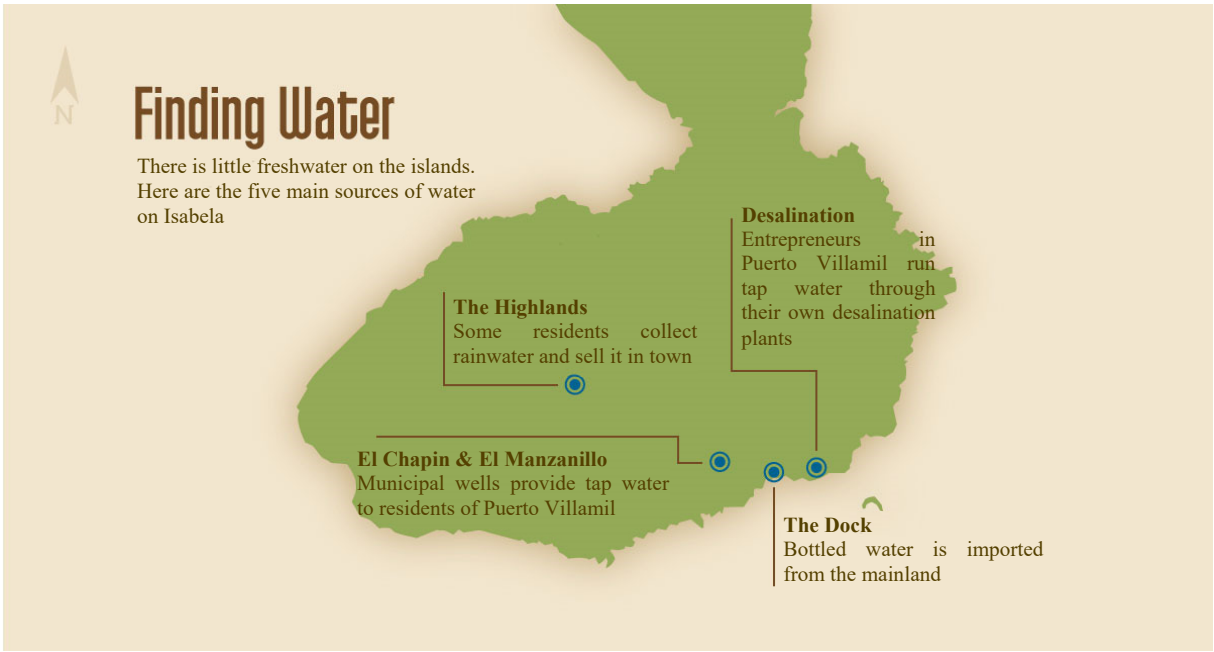

FIGURE 2: Location of the main water sources on Isabela Island (Living Galápagos, 2015)

2.2 Contamination of water supply

Studies on the quality of tap water show evidence of bacteriological and a possible chemical contamination at the municipal extraction locations. This is possibly caused by a lack of sanitation protocols, which causes water to be in contact with contaminated elements along the pipelines (Guyot-Téphany et al., 2012).

Liu (2011) states in her report that despite the presence of pathogens in the water during extraction, the biggest contamination source is the poor storage conditions in households. The absence of chlorine disinfection practices and, not cleansing the reservoirs permanently, causes bacteria in the water to multiply. As a result, the population is vulnerable to an outbreak of stomach and intestinal diseases. An outbreak already occurred in 2006 where water analysis, traced the origin of the infection to inadequate water treatment (Guyot-Téphany et al., 2012).

A third issue is the salinity of the tap water. A study carried out in 2007 by López et al., revealed that the concentration of salt in the municipal tap water systems in Isabela greatly exceeded the level recommended for human consumption Figure 3. For human consumption water must contain less than 1000 mg of salt per litre.

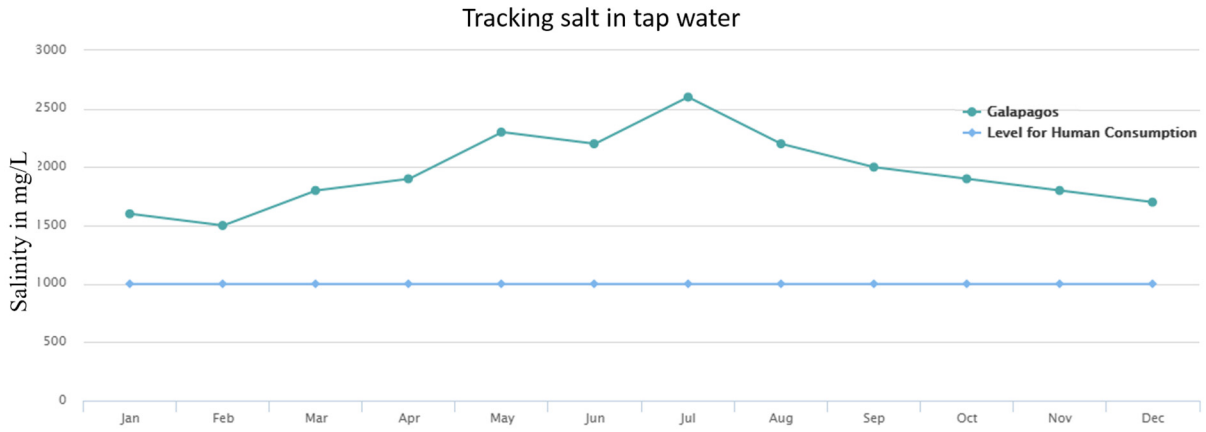

FIGURE 3: Salinity concentration in municipal tap water systems in the Galápagos (Walsh et al., 2010)

2.3 Consequences of the current water supply scheme

In 2009, it was estimated that approximately 70% of diseases in Puerto Villamil resulted from consumption or exposure to contaminated water. Common water-related illnesses include gastrointestinal problems such as diarrhea and gastritis, fungal skin infections and urinary tract infections. Young children (1-4 years of age) are most affected by the effects of tap water and the related health issues, because their immune systems are under-developed, they practice poor hygiene, and tend to experience higher exposures to contaminated sources of water (Walsh et al., 2010). Similar illnesses, which were documented around the world in the past, due to high levels of sodium in drinking-water (WHO, 2003), are likely to happen in the island as a result of the current situation.

In an attempt to prevent this, boiling water is a common practice among the inhabitants. In Isabela, 41% of the population boil the tap water to prevent diseases when using it for drinking and cooking. This is also done in Santa Cruz and San Cristobal, as shown in Figure 4. Household owners also collect rain water from roofs, although this practice has decreased due to the fact that in the past, roofs were typically made of fibercement with asbestos, which are known to cause serious health hazards in humans. A third option is to obtain purified water from a local private water desalination business.

Although this is the preferred option among villagers, it is also the most expensive compared to the previous methods (Guyot-Téphany et al., 2012).

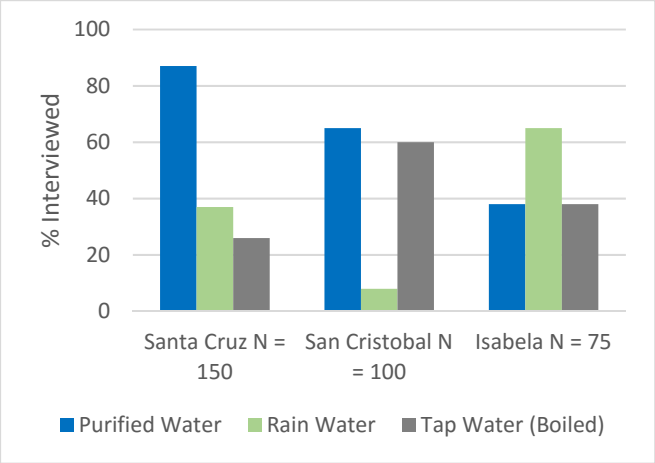

FIGURE 4: Type of water used for human consumption (modified fom Guyot-Téphany et al., 2012)

Contrary to the belief that a limited resource will cause a more responsible use, low quality water creates a culture of wastefulness among the citizens as it has almost no economic value. For example, 61% of interviewed residents who have a tank in Santa Cruz, as well as 47% in San Cristobal and 21% in Isabela, confirm that they allow their tank to overflow once it fills (Guyot-Téphany et al., 2013). In addition, failures in the current supply network are also major causes for water wastage. It is estimated that the volume of water wasted or lost in the system is higher than the volume of water actually consumed (Guyot-Téphany et al., 2012).

Furthermore, activities related to extraction, distribution and use of water resources from aquifers in Isabela rely directly or indirectly on the use of fossil fuels; Gasoline is used in tanker trucks to distribute water to households and, in electric powered storage infraestructures, which were built to bypass the water supply restrictions in the island. In addiion, approximately 5.370 m³ of bottled water is imported annually from the mainland to cover the influx of tourist and supply to local demand (CEPROEC-IAEN and SENPLADES, 2014). Considering that 94% of energy generated in Galápagos comes from fossil fuels (CEPROEC-IAEN and SENPLADES, 2014), the scheme under which the water supply system operates is detrimental in terms of sustainability efforts in the island, and it is certainly in contrast to the government´s plan to eliminate the use of fossil fuels in the Galápagos in the future (MEER, 2015).

3. GEOLOGICAL SETTING OF THE GALÁPAGOS

The Galápagos Islands are an archipelago of 13 main islands, and 48 small islands and islets that belong to the Republic of Ecuador (Neall and Trewick, 2008). They are located on top of a hotspot on the Nazca Plate in the eastern Pacific Ocean, 973 km off the west coast of Ecuador. The Islands are among the most active oceanic volcano groups in the world (Simkin, 1984).

The archipelago is the result of hotspot activity 100 km south of the Galápagos Spreading Center (GSC), a mid-ocean ridge separating the Cocos and Nazca plates (Figure 5). The islands emerge from a broad submarine volcanic platform that marks the western end of the aseismic Carnegie Ridge (Geist et al., 1998). The GSC is migrating north-west away from the hotspot and is thought to have overlain the hotspot around 8 million years ago (Hey, 1977). The proximity of the hotspot and the spreading ridge creates a complex geochemical interaction that strongly affect the composition of lavas from the ridge (Schilling et al., 1976; Verma et al., 1983; in Geist et al, 1998).

Holocene volcanism is present throughout the archipelago. Each major island consists of a single large volcano, which have been active historically, with the exception of the largest island, Isabela, which consists of six volcanoes (Geist et al., 1995). The archipelago has distinct petrologic and volcanologic subprovinces defined by regional differences in the morphologies of the volcanoes (McBirney and Williams, 1969). In general, the lavas tend to be more alkaline and enriched isotopically to the east, north, and south from the central east-west axis of the archipelago, but the central and southern

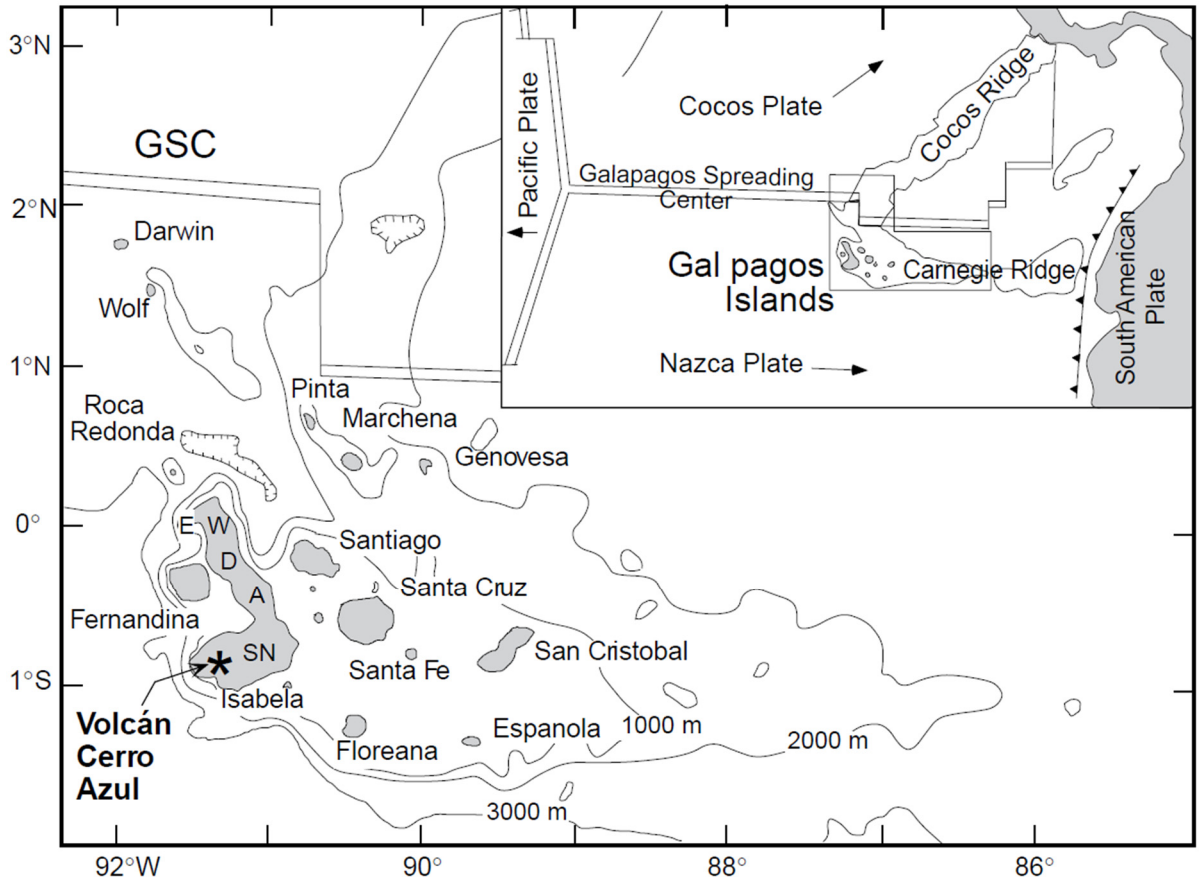

FIGURE 5: Bathymetric map of the Galápagos archipelago. Abbreviations for the six volcanoes of Isabela Island are: E, Ecuador; W, Wolf; D, Darwin; A, Alcedo; SN, Sierra Negra; CA, Cerro Azul. GSC, Galápagos Spreading Centre (Geist et al, 1998)

volcanoes have erupted basalts with unusually great diversity in trace element compositions (Geist, 1992). Chemical and isotopic data indicate that the Galápagos magmas are generated as an undegassed deep mantle plume rises and mixes with magmas derived from relatively depleted asthenospheric mantle (White et al., 1993; Graham et al. 1993). Diffuse hydrothermal phenomena and fumarolic activity occur at several volcanoes throughout the archipelago (Simkin, 1984).

3.1 Isabela

Isabela is the largest island of the Galápagos archipelago with an area of 4,640 km^2 (Figure 6). The hotspot is supposedly centred under the island, which gives origin to six active volcanoes spread across its surface. Along with Fernandina volcano which is located in the neighbouring island with the same name, these two land masses comprise the seven western Galápagos shield volcanoes. The town of Puerto Villamil is located at the southeast point of the island. Autochthonous wildlife and vegetation prevail in the areas around the volcanoes, including the world's largest population of giant tortoises. As is the case

FIGURE 6: Isabela Island view from space (Source: NASA, 1988)

with the rest of the archipelago, almost the entire island is a National Park, subject to environmental regulations and limited public access to maintain its status as a World Natural Heritage site, granted by the United Nations Educational, Scientific and Cultural Organization (UNESCO) in 1978.

Geothermal activity has been documented in the past years around three volcanoes in Isabela: Alcedo, Sierra Negra, and Cerro Azul (Geist et al., 1994; Goff et al., 2000; Naumann et al., 2002). These geothermal prospects shown in Figure 7 were selected based on the available data, and will be discussed in the following sections.

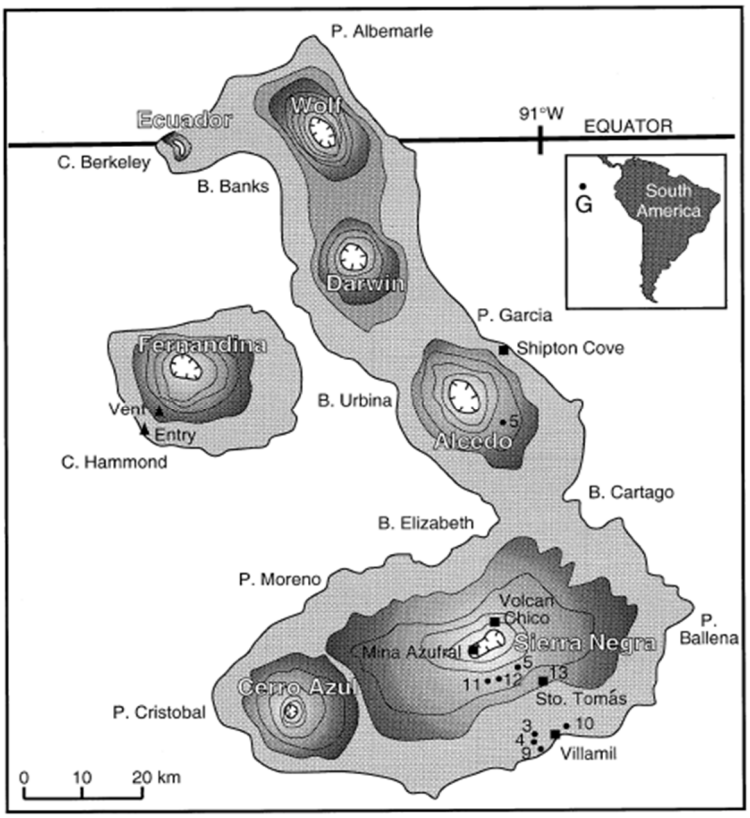

FIGURE 7: Map location of shield volcanoes on Isabela and Fernandina Islands, Galápagos Archipelago. Contour interval is 200 m (Goff et al, 2000)

3.2 Alcedo

Alcedo, located in the centre of Isabela, is the only active Galápagos volcano known to have erupted rhyolite as well as basalt. Its caldera is 7-8 km wide and has a maximum depth of 270 m. This geothermal prospect stands at 1128 m.a.s.l., and its one and only known eruption occurred sometime between 1946 and 1960 from its southern flank, according to aerial photographic evidence (Geist et al., 1994).

The geological setting is characterized by an old basaltic eruptive phase, an intermediate age rhyolite phase, and a young basaltic phase. Several hydrothermal explosion craters followed by fumarolic activity in the eastern zone and, the evidence of subsurface fracture networks, denotes that hydrothermal activity in the area is transient and fault controlled (Goff et al, 2000). Based on surface exploration studies and hydrogeochemical data presented by Goff et al. (2000), Alcedo is likely to host a high-temperature geothermal system. A preliminary conceptual cross-section of the geothermal model is shown in Figure 8.

Reservoir temperatures are estimated between 260 and 320°C, and may circulate as deep as 1 km based on gas geothermometry. The presence of high water content and predominance of reduced sulphur supports the existence of a liquid-dominated system. The reservoir is under a vapour-rich cap and contains neutral-chloride rich fluids. These are composed primarily of local meteoric water infiltrating the caldera and degassed magmatic components from shallow, compound rhyolitic intrusions (Geist et al., 1994; 1995). Permeability is enhanced by a fault controlled system and explosive rhyolitic events. Basaltic eruptions post-dating the rhyolites may add additional heat and magmatic volatiles to the system (Goff et al., 2000). Considering the size of the geothermal anomaly in Alcedo, an estimated power output of 150 MW can likely be obtained if an equivalent volume (15 m^3/s) of flashed steam is generated from geothermal wells at a separation temperature of 180°C (Goff et al., 2000).

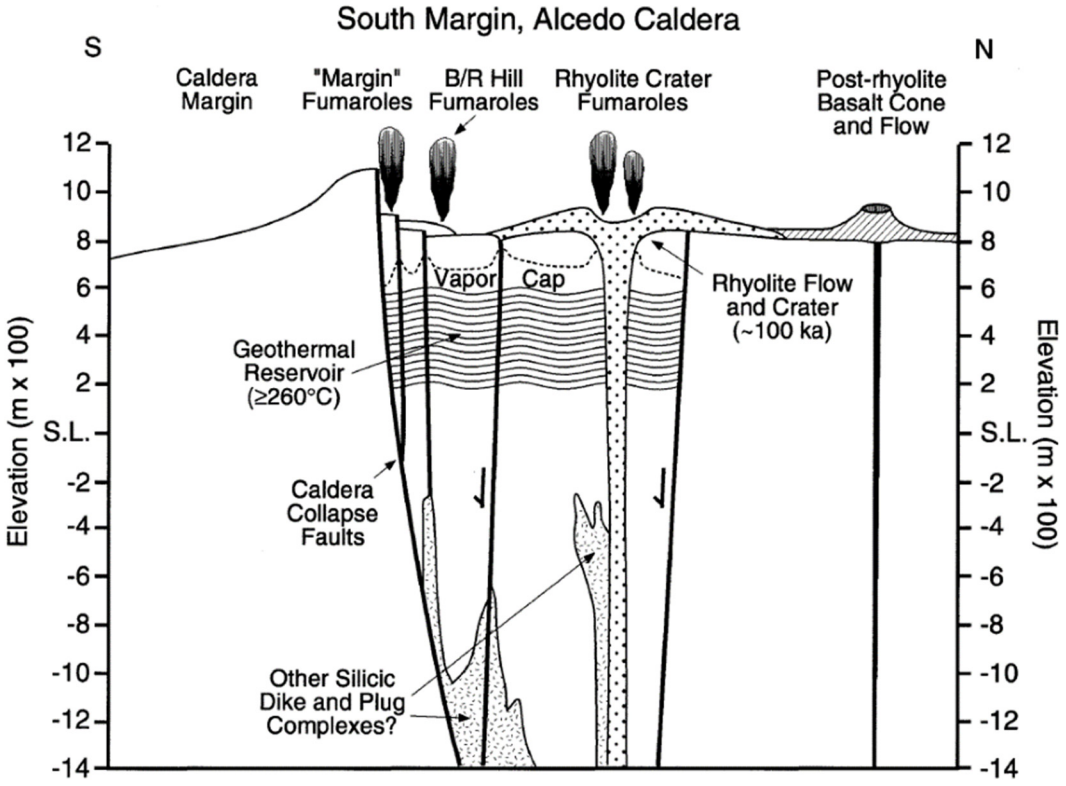

FIGURE 8: Conceptual cross-section of hydrothermal activity in southern sector of Alcedo volcano, Galápagos (Goff et al, 2000)

3.3 Sierra Negra

With a caldera of 7 x 10 km and elevation of 1124 m.a.s.l., Sierra Negra is the largest and most active shield volcano in the archipelago, located at the south eastern end of Isabela Island. It collides with Alcedo to the north and Cerro Azul to the west. The last eruption of Sierra Negra Volcano was registered in October 2005, after 26 years of relative low activity (IGEPN, 2015).

Geothermal manifestations are mainly observed in two particular areas: In a fissure where a parasitic cone named Volcán Chico is located, and in a high temperature fumarole field named Mina Azufral. Activity in this location is mainly fault controlled, creating particular high temperature fumaroles in the range of 110- 210°C, which are associated with sulphur deposits. Both sites were studied by Colony and Nordlie (1973), and Delaney et al. (1973).

Goff et al. (2000) elaborated a conceptual model of hydrothermal activity in the western sector of Sierra Negra based on surface exploration activities and hydrogeochemical data. A conceptual cross-section is shown in Figure 9.

The presence of relatively small basaltic magma intrusions at under 5 km depths are inferred within the conceptual model. The heat from these magmatic bodies may have created a ‘blind geothermal system’ that circulates the western moat, as no surface hydrological evidence such as hot springs is visible to confirm the existence of this theory. Detailed visual reconnaissance of the fumarole field at Mina Azufral suggest that the source of magma and the fault structure has remained relatively unchanged over the last 100 years (Goff et al., 2000).

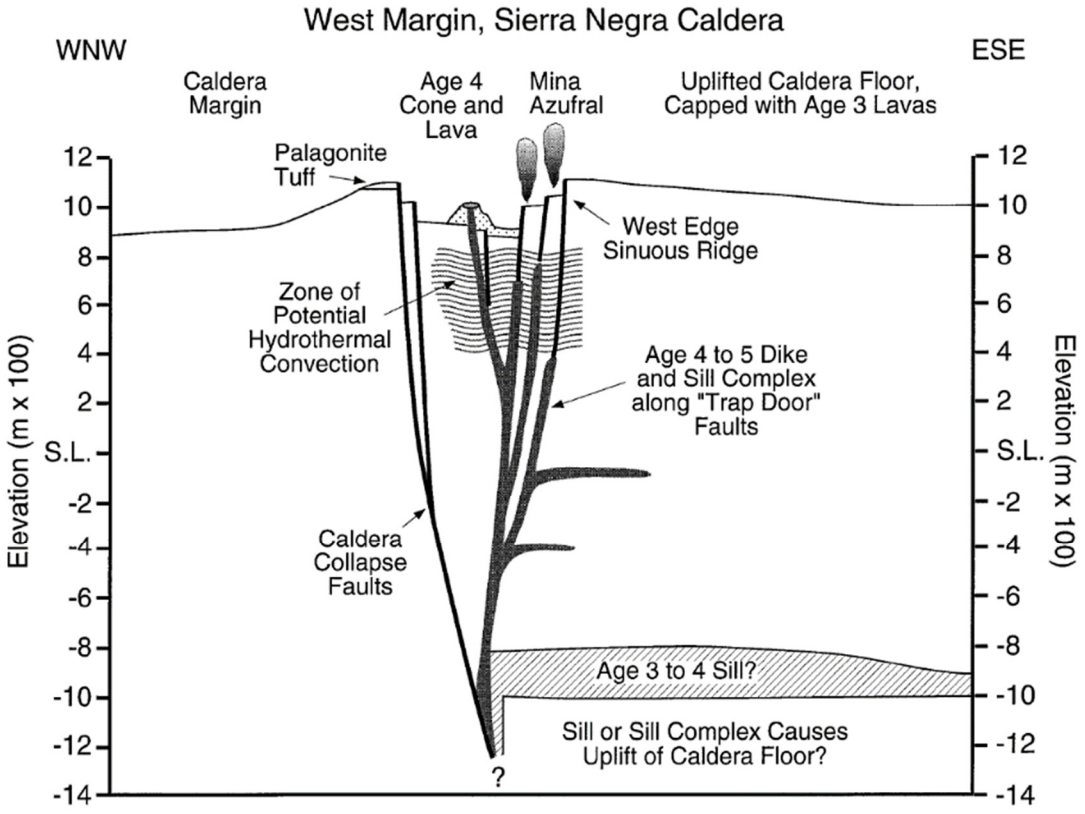

FIGURE 9: Conceptual cross-section of hydrothermal activity in western moat of Sierra Negra volcano, Galápagos (Goff et al, 2000)

Gas geothermometry indicates an apparently shallow decompression of magma. This statement is supported by the presence of high temperature fumaroles and a predominant release of SO_2. Shallow hydrothermal fluids mix with magmatic gases before reaching the surface. Nonetheless, not enough heat is provided by basaltic dikes to sustain a vigorous hydrothermal convection system within the Sierra Negra caldera (Goff et al., 2000).

3.4 Cerro Azul

Cerro Azul Volcano forms the south west end of Isabela Island (Figure 7). It rises up to 1640 m.a.s.l. and is second in elevation only to Wolf Volcano (1710 m.a.s.l.). It is also the second most active volcano after Sierra Negra, with an average of one eruption every 6.5 years (IGEPN, 2015).

Naumann and Geist (2000), and Naumann et al. (2002), provide detailed information on the eruptive history, growth rate, and morphologic development; as well as detailed major, trace and isotopic analyses from Cerro Azul. Clear evidence of explosive hydrovolcanic activity has been documented from Hawaiian-style eruptions in the vents on the caldera floor and southern summit rim (Figure 10).

A cross-section of the caldera denotes an area of 4,2 x 2,2 km, the smallest among the western Galápagos shield volcanoes. Nevertheless, its depth (450 m) almost doubles the one of Alcedo, and extends nearly 4 times Sierra Negra caldera´s depth (Naumann et al., 2002). No geochemical information on hydrothermal fluids that would help to determine the presence or lack of a geothermal system was available when this report was written.

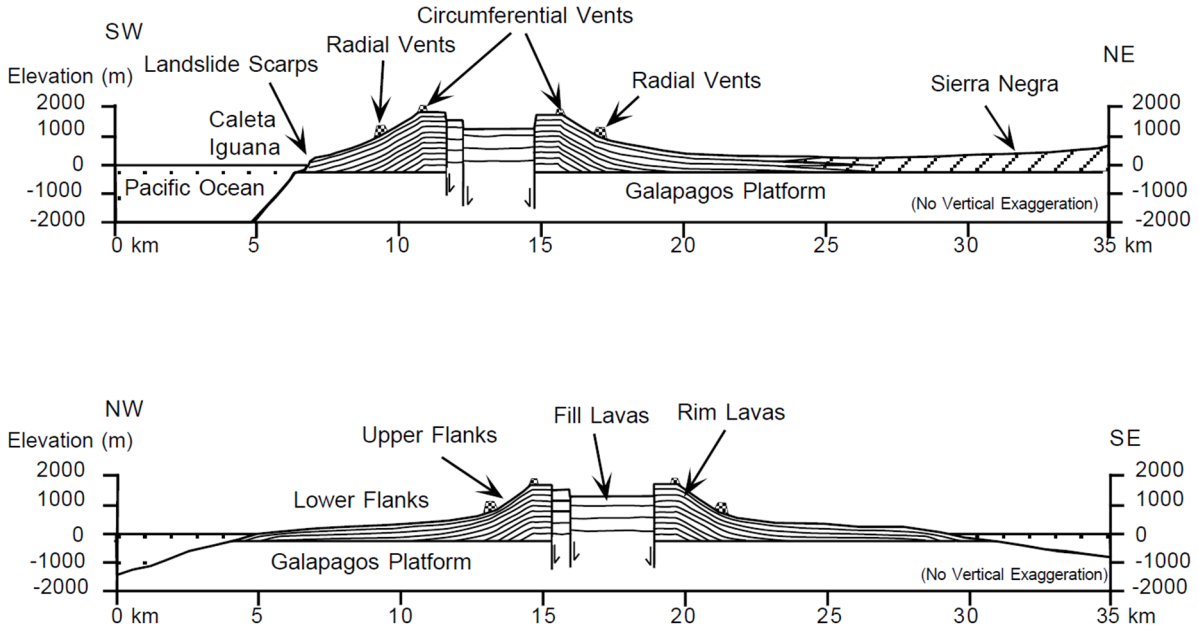

FIGURE 10: Schematic geologic map of Cerro Azul showing cross-sections and internal structure (Naumann et al, 2001)

4. DESALINATION PROCESS

4.1 Overview and current status

The desalination of sea water is the separation of nearly salt-free fresh water from sea or brackish water, where the salts are carried in the rejected brine stream and disposed of back in the sea. A desalination process can be based on thermal or membrane separation methods. The thermal separation techniques consist of evaporation followed by condensation of the formed water vapour, and, freezing followed by melting of the formed water ice crystals. The former process is the most used and nearly in all cases, coupled with power generation units which may be based on steam or gas turbine systems. The evaporation of the brine can be achieved by either boiling or flashing techniques.

Presently, the desalination industry is experiencing a vast expansion around the globe. This is because of an increase in water demand and higher cost of fresh water from natural resources. Although thermal desalination has been increasingly taken over by membrane processes during the last 15 years, it still accounts for 30% of the total desalinated water produced globally (Ghaffour et al., 2015). Multi Stage Flashing (MSF) and Multiple Effect Distillation (MED) technologies dominate the market in thermal desalination.

4.2 Developments in MSF

Since it was first used in 1950, MSF has gone through a series of improvements in its initial design, as the technology advanced and experience was gained from its operation (El-Dessouky and Eltouney, 2002). MSF is derived from Single Stage Flashing (SSF), where seawater is evaporated by reducing the pressure, as opposed to raising the temperature. The latent heat released by the condensing water vapour at each stage gradually raises the temperature of the incoming seawater. The SSF system includes the brine heater and the flashing chamber, which contains the condenser/preheater tubes, the demister, the brine pool, and the collecting distillate tray.

Modifications to the original design, from Single Stage Flashing, to Once Through MSF, to Brine Mixing MSF, and finally to MSF with Brine Recirculation and a Heat Rejection Section, lead to an overall increase of the thermal performance ratio and reliability of the system. Figure 11 shows the most distinctive features and drawbacks of each configuration.

The Three Stage Heat Rejection Brine Circulation (MSF-M) process is currently the industry standard. It combines the previous MSF and MSF-OT features to reduce energy losses and significantly increase the overall system performance (El-Dessouky and Eltouney, 2002). A scheme of MSF-M desalination plant is shown in Figure 12.

Further developments in MSF technology are mainly focused on continuous improvements, such as maximizing the profitability of operation, thermal performance ratio, and optimizing the design and operating parameters. Likewise, replacing non-renewable fossil fuels as energy input in the desalination process, with nuclear energy and renewables in the future.

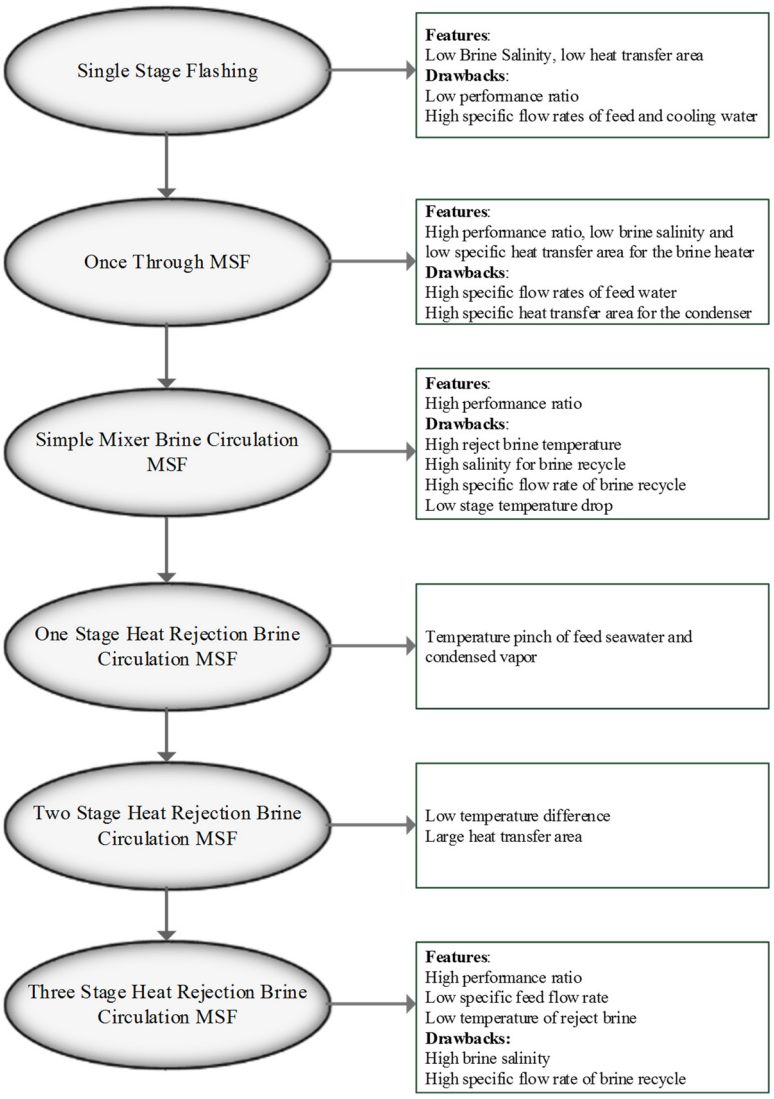

FIGURE 11: Performance summary of various MSF configurations (modified from El-Dessouky and Eltouney, 2002)

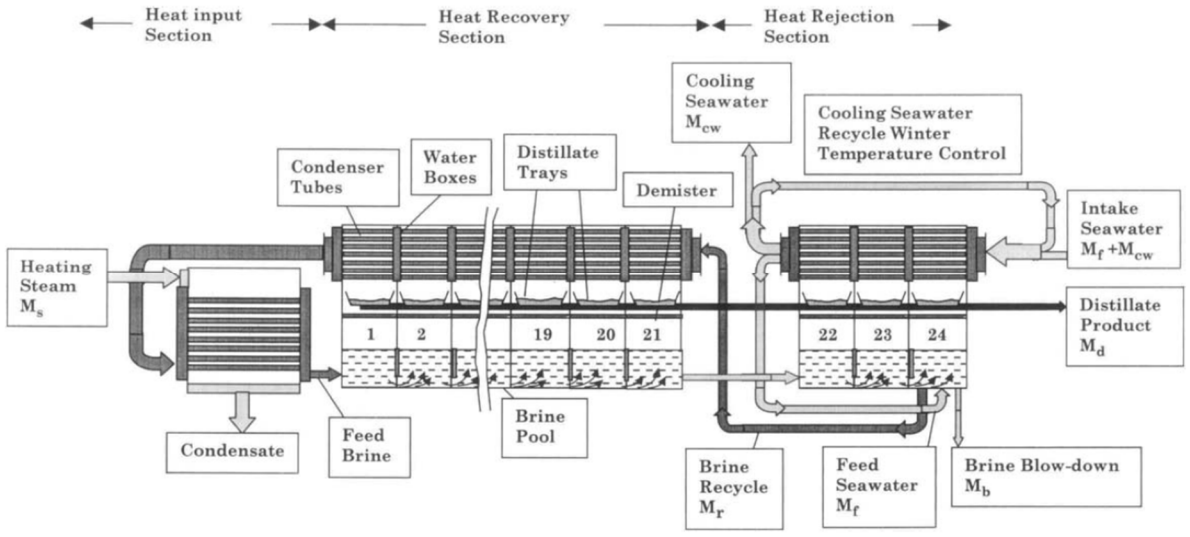

FIGURE 12: Multistage flash desalination with brine recirculation (MSFM) (El-Dessouky et al, 1999)

4.3 RE-driven desalination plants

The present installed desalination capability using RE is negligible compared to the world's total capacity, despite the fact that several small-scale RE-driven desalination plants have been installed worldwide and most of them have been successfully operated under very simple maintenance (Goosen et al, 2014). In the case of geothermal energy, one of the most documented case studies is the Kimolos Geothermal Desalination Project. Built in 1999, a Multiple Effect Distillation unit produced 80 m^3/h of potable water, utilizing geothermal steam at a wellhead temperature of 61°C, for the inhabitants of the Kimolos Island (Karytsas et al., 2004).

Although renewable desalination systems cannot presently compete with conventional technologies in terms of water costs (mostly due to the low price of fuels), they remain applicable for remote and arid areas with limit water access and are likely to represent a feasible solution at a large scale in the near future (Ghaffour et al., 2015).

5. THERMODYNAMIC MODELLING AND EXERGY ANALYSIS

To estimate the feasibility of water desalination through the use of geothermal energy, a thermodynamic model and exergy analysis of a SSF-G desalination system were done to study the physical and chemical behaviour of this particular system configuration. The thermodynamic modelling framework helps to describe and validate available data, and to extrapolate with reasonable confidence outside the range of available data. On the other hand, an exergy analysis will help identifying the causes, locations and magnitude of the system inefficiencies associated with chemical reaction, heat transfer, mixing, and friction. It also provides the true measure of how far the system departs from its equilibrium state (Dincer and Rosen, 2007).

The Single Stage Flash configuration was chosen in this study based on its relative simplicity and the daily demand of fresh water from Isabela Island, which is estimated at 276 m^3. Although, the MSF-M is the most efficient in terms of performance, the overall upfront costs of adding more flashing stages, a recirculation brine system and a heat rejection stage, will most likely compromise the project´s economic feasibility when faced with such a low demand of fresh water. MSF is commonly more suitable for large scale distillate production (over 100.000 m^3).

5.1 Description of work

The main objectives of this project are to:

- Develop a thermodynamic model and exergy analysis of a Single Stage Flash (SSF) desalination system;
- Simulate the separation of nearly salt-free fresh water from sea in Isabela Island using geothermal brine as the primary heat input source;
- Simulate the production of electricity for the operation of the desalination cycle, using geothermal steam from the separator unit;
- Determine the performance parameters of the system, i.e. the total mass and salt balances, rate equations for the heat transfer units, as well as energy balances for the brine heater and the condenser.

The Engineering Equation Solver (EES) software was used for developing and analysing the thermodynamic model of energy and exergy flow. The simulation was based on overall heat transfer coefficients, salt balances and, the following design parameters described below.

5.2 Design parameters

Design parameters for the geothermal single stage flash were selected based on information from the geothermal resource in Alcedo. Normal operating conditions for the geothermal and desalination cycle were obtained from literature reviews. Seawater properties (temperature and salinity) were assumed based on the geographical location. The following parameters were used for the thermal design:

Geothermal input

- Reservoir temperature was estimated at 260°C.
- Flashed steam mass flow was estimated at 15 kg/s.
- Separation temperature was estimated at 180°C.
- All pressure and heat transfer losses were neglected.

Sea water properties and distillate water demand

- Seawater temperature was estimated at 20°C.
- Salinity of seawater was estimated at 42.000 ppm.
- Desalination capacity of the system was set to 276 m^3/day.

Desalination plant

- Constant and equal specific heat for all liquid streams.
- Negligible effect of non-condensable gases on the heat transfer process.
- Negligible effects of the boiling point rise and non-equilibrium losses on the stage energy balance; however, their effects are included in the design of the condenser heat transfer area.
- The distillate product was assumed to be salt-free.
- The maximum attainable concentration of the rejected brine, X_b, was 70.000 ppm. This value was imposed by scale formation limits of $CaSO_4$.

5.3 Process description

The layout for the SSF-G process shown in Figure 13. The main elements include the brine heater and the flashing chamber, which contains the condenser/preheater tubes, the demister, the brine pool, and the collecting distillate tray. The main elements of the geothermal desalination system include the separator to obtain steam and brine, a turbine to produce electricity required by the desalination process, and a condenser to maximize the turbine efficiency. The geothermal fluid can be supplied from a single well in the Alcedo geothermal field. The characteristics in the well are roughly estimated based on the existing data.

The geothermal brine coming from a separator unit at a saturation pressure of 10 bar, and a temperature of 180°C enters the brine heater on G3, while the feed seawater enters the other side in point 2. The geothermal feedwater exits the heater and is injected back into the reservoir. The heat transfer that occurs in the brine heater increases the feed seawater temperature to the top brine temperature in point 4. The hot brine enters the flashing stage at a pressure lower than the saturation pressure of the brine. This allows a free flow of the stream across the system, without the aid of pumping power. As the brine circulates through the flashing chamber, heat is transferred by evaporation of a small portion of the brine inside the evaporator. The remaining brine carrying the gained salinity is returned back to the sea in point 7. The formed vapour flows through the demister pad, which prevents product contamination from brine droplets entrained with the flashed off vapour. In point 5, the vapour releases its heat as it condenses on the seawater condenser/preheater tubes. The condensed vapour, which results in high purity distillate water, is collected in the distillate tray, and then exits the system at stage 6. One of the heat recovery features in the SSF process is that it transfers

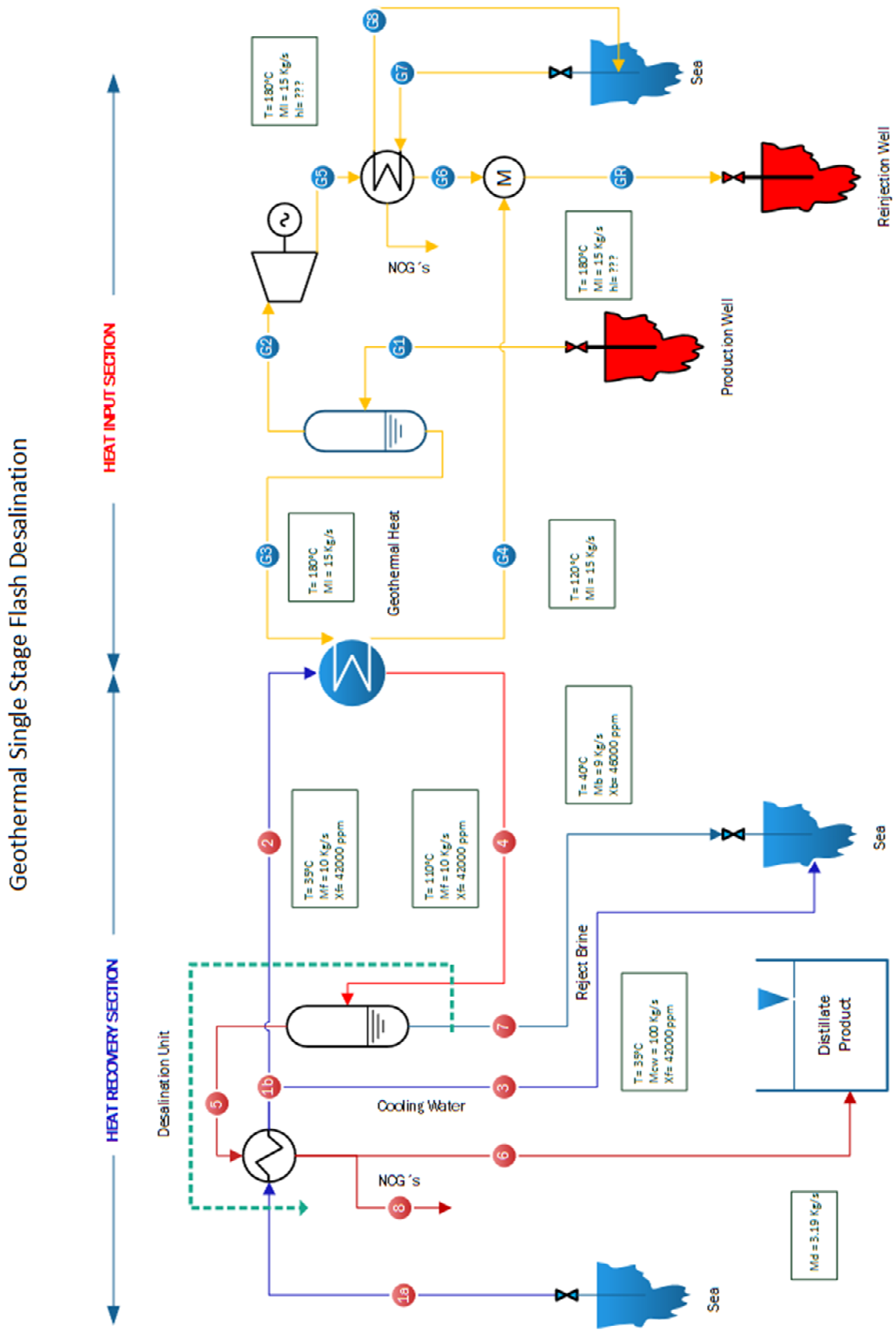

FIGURE 13: Process diagram for the SSF-G system

the heat of condensation to the intake seawater. As a result, seawater is preheated from its natural state to the feed temperature. The cooling seawater removes the excess heat added to the system in the brine heater and is rejected back to the sea after exiting the condenser in point 7.

The feed seawater undergoes a pre-treatment process which includes de-aeration and addition of antiscalant and foaming inhibitors before flashing. The distillate water produced by the SSF plant follow a potabilization process to raise the calcium and bicarbonate contents of the water and adjust the pH to make the product suitable for human consumption. Fresh water from the distillate is stored in tanks or injected directly into the municipal distribution network.

5.4 Thermodynamic modelling

The thermodynamic model for the SSF process is shown in Figure 14, and consists of two main sections: heat input, and heat recovery. In the heat input section, the geothermal liquid phase at T_{G3} enters the brine heater, where it releases its sensible heat to the feed seawater. This energy increases the temperature from T_2 to the top brine temperature T_4. The terminal temperature difference caused by the heat exchange process between the geothermal brine and the effluent sea water brine, is represented by TTD_h. The type of chemical additive that is used to control scale formation dictates the upper limit on T_4. For acid and modern chemical additives, the limit on T_4 is 120°C and for polyphosphate the limit is 90°C (El-Dessouky and Eltouney, 2002). In the heat recovery section, the feed seawater flows into the flashing chamber. This process is represented by the stage temperature drop, ΔT_{st}, where part of the sensible heat is converted into latent heat by the evaporation of the brine pool. The latent heat is released to the intake seawater as the vapour condenses in the seawater condenser/preheater tubes, increasing the temperature from T_{1a} to the feed seawater temperature T_2. The temperature difference of the condensing vapour and the seawater leaving the condenser, is shown as TTD_c.

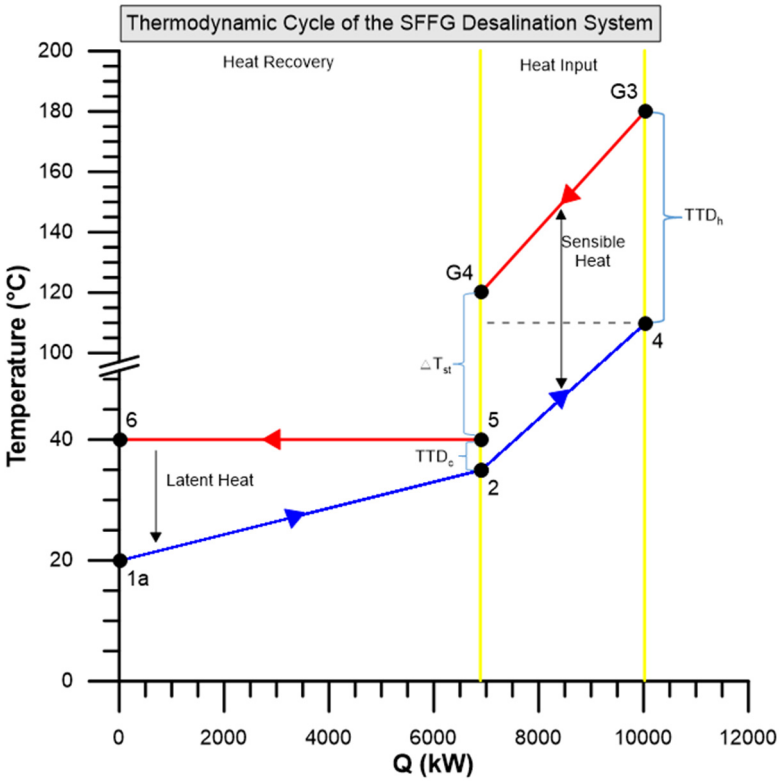

FIGURE 14: Thermodynamic model of the SSF-G system

Recovery of the latent heat by the feed seawater improves the overall efficiency of the desalination process and controls the saturation pressure inside the flashing chamber. Distillation results from the condensation of the feed seawater.

Thermodynamic losses occur during the SSF. These are caused by the boiling point elevation, the non-equilibrium allowance, and the temperature drop corresponding to the pressure drop in the demister pad and during condensation.

5.5 Thermodynamic relations

A simplified thermodynamic model for the Geothermal Single-Stage Flash (SSF-G) process is presented below and will provide a first approach into a more detailed mathematical model to be developed in the future as more accurate data becomes available. The total mass and salt balance equations are given by:

$$\dot{m}_f = (\dot{m}_b + \dot{m}_d) \tag{1}$$

$$X_f \dot{m}_f = X_b \dot{m}_b \tag{2}$$

where $\dot{m}$ is the mass flow rate, X is the salt concentration and the subscripts b, d, and f refer to the brine, distillate, and feed water, respectively.

The brine heater and condenser energy balances are given respectively by:

$$\dot{m}_{G3}(h_{G3} - h_{G4}) = \dot{m}_2(h_4 - h_2) \tag{3}$$

$$\dot{m}_6(h_5 - h_6) = \dot{m}_{1a}(h_{1b} - h_{1a}) \tag{4}$$

where h is the enthalpy of the fluid and the subscripts G3, G4, 1a, 1b, 2, 4, 5 and 6, refer to the stage number.

The heat transfer rate equations for the brine heater is:

$$Q_h = U_h A_h (LMTD)_h \tag{5}$$

where

$$(LMTD)_h = \frac{(T_{G3} - T_4) - (T_{G4} - T_2)}{\ln\big((T_{G3} - T_4/T_{G4} - T_2)\big)} \tag{6}$$

The heat transfer rate equation for the condenser is:

$$Q_c = U_c A_c (LMTD)_c \tag{7}$$

where

$$(LMTD)_c = \frac{(T_5 - T_{1b}) - (T_6 - T_{1a})}{\ln\big((T_5 - T_{1b}/T_6 - T_{1a})\big)} \tag{8}$$

In the above system of equations, A is the heat transfer area, U is the overall heat transfer coefficient, and T is the temperature. The subscripts c and h refer to condenser, and brine heater respectively.

The unit thermal performance ratio, defined as the mass ratio of fresh water produced per unit mass of heating steam, is obtained by:

$$PR = M_6/M_{G3} \tag{9}$$

Single-flash cycle

The flow rate of the steam and brine are defined by mass and heat balance of the separator as follows:

$$\dot{m}_{G1} = \dot{m}_{G2} + \dot{m}_{G3} \tag{10}$$

$$\dot{m}_{G1} h_1 = \dot{m}_{G2} h_2 + \dot{m}_{G3} \tag{11}$$

where $\dot{m}$ and h are the mass flow and enthalpy of the stream. The subscript numbers denote the state position of stream in Figure 13.

The turbine power production is:

$$\dot{W}_{turb} = \dot{m}_{G2}(h_{G2} - h_{G5}) \tag{12}$$

$$\eta_{turb} = \frac{(h_{G2} - h_{G5})}{(h_{G2} - h_{G5s})} \tag{13}$$

where h_{G5} and h_{G5s} are the enthalpy values at the turbine exit states for actual and isentropic processes, respectively. For the condenser, the heat rejected by cooling water is:

$$\dot{Q}_{Cond} = \dot{m}_{G2}(h_{G5} - h_{G6}) \tag{14}$$

The mass flow of cooling water is defined by:

$$\dot{m}_{CW} = \frac{\dot{Q}_{Cond}}{(h_{G8} - hG_7)} \tag{15}$$

where h_7 and h_8 are the enthalpies of cooling water at the inlet and outlet of condenser.

5.6 Exergy analysis

The concept of exergy relates to the maximum work output that could theoretically be obtained from any system relative to given surroundings. It is often referred to the state of the surroundings as the dead state because when fluids are in thermodynamic equilibrium with the surroundings there is no potential for doing work, and the fluid may be considered "dead" (DiPippo, 2004).

Disregarding kinetic and potential energy changes, the specific flow exergy of a geothermal fluid at any stage can be calculated from

$$E = \dot{m}\big(h - h_{dead} - T_{dead}(s - s_{dead})\big) \tag{16}$$

where T_{dead} is the environment (dead state) temperature, h and s are the enthalpy and the entropy of the geothermal fluid at the specified stage, and h_{dead} and s_{dead} are the corresponding properties at the restricted dead state (Kanoglu, 2002).

Exergetic Efficiencies

The definition is used in this report is called rational efficiency and defined by Kotas (1985) as the ratio of the exergy recovered to the exergy supplied to the system or process:

$$\eta_e = \left(E_{desired}/E_{input}\right) \tag{17}$$

$$E_{input} = E_{output} + E_{destroyed} \tag{18}$$

$$E_{output} = E_{desired} + E_{waste} \tag{19}$$

where E_{desired} = Sum of desired exergy outputs (net positive work by the system);
$E_{\text{destroyed}}$ = Exergy rate lost in the system as a result of irreversibility;
E_{waste} = Exergy exiting the system which still has capacity to do work.

When this concept is applied to a power plant as a whole, the overall exergetic efficiency reduces the ratio of the net power output to the exergy of the motive fluid serving as the energy source for the plant (DiPippo and Marcille, 1984). Consequently; the exergetic efficiency for the single flash cycle based on the two phase fluid exergy input to the plant can be calculated as:

$$\eta_{e\_overall\_SF} = \left(\dot{W}_{net\_}SF/E_{G1}\right) \tag{20}$$

where the $\dot{W}_{net\_}SF$ is the net power output of single flash cycle and E_{G1} is the exergy rate of two phase geothermal fluid in stage 1.

The exergetic efficiency of the single flash condensing turbine, can be calculated as:

$$\eta_{\varepsilon\_SF\_Turb} = \left(\dot{W}_{SF\_Turb}/E_{G2} - E_{G5}\right) \tag{21}$$

The difference between the numerator and denominator in Eq. (21) gives the exergy destruction in the turbine.

$$I_{SF\_Turb} = (E_{G2} - E_{G5}) - \dot{W}_{SF\_Turb} \tag{22}$$

The brine heater and condensers in the desalination plant are essentially heat exchangers designed to perform different tasks. The exergetic efficiency of a heat exchanger may be measured by the increase in the exergy of the cold stream divided by the decrease in the exergy of the hot stream (Wark, 1995). Applying this definition to the condenser in single flash cycle, the following equation is obtained:

$$\eta_{\varepsilon\_cond\_SF} = \frac{E_{G8} - E_{G7}}{E_{G5} - E_{G6}} \tag{23}$$

where the exergy rates are given in Table 1. The difference between the numerator and denominator in Equation 23 gives the exergy destruction in the condenser:

$$I_{cond\_SF} = (E_{G5} - E_{G6}) - (E_{G8} - E_{G7}) \tag{24}$$

Nonetheless, the exergy drop of the working fluid across the condenser can be expressed as the exergy destruction in the condenser. That is, the exergy gained by the cooling water is not considered (Kanoglu, 2002).

The exergetic efficiency of the heat exchangers in the desalination cycle is calculated as below:

$$\eta_{\varepsilon\_brine\_\mathrm{H}} = \frac{E_4 - E_2}{E_{G3} - E_{G4}} \tag{25}$$

$$\eta_{\varepsilon\_cond\_DS} = \frac{E_{1b} - E_{1a}}{E_5 - E_6} \tag{26}$$

The exergy balance for the desalination and the single flash combined system can be written as:

$$E_{in} = E_{out} + E_{des} + E_{loss} \tag{27}$$

where

$$E_{in} = E_{1a} + E_{G1} + E_{G7} \tag{28}$$

$$E_{out} = \dot{W}_{SF\_Turb} \tag{29}$$

$$E_{loss} = E_3 + E_6 + E_7 + E_{G4} + E_{G8} \tag{30}$$

5.7 Results

The results from thermodynamic calculations and exergy analyses of the proposed system were established in the EES software. In Table 1, temperature, pressure, mass flow, enthalpy, entropy and exergy rate data for geothermal fluid, working fluid, and cooling water are given according to their stage numbers specified in Figure 13.

For geothermal fluid, the thermodynamic properties of water were used. The thermodynamic properties of the working fluid, sodium chloride, were obtained from the EES software. The temperature of the sea brine at the exit of the brine heater (stage 4 in the process diagram) was

restricted by the calcium sulphate saturation point and should be in the range 90-110°C to prevent calcium deposition inside the flashing chamber. At the other exit of the brine heater (stage G4 in the process diagram), the temperature was restricted by the silica amorphous saturation point and should be in the range 70-120°C to prevent the silica deposition inside the mixer (El-Dessouky and Eltouney, 2002). The data listed in Table 1 was created by the thermodynamic design model when running it in the EES software.

TABLE 1: Results from thermodynamic calculations and exergy analyses of the proposed system

Stage	**Fluid**	**Phase**	***Salinity***	$\dot{m}$	***T***	***P***	***h***	***s***	***E***
N°			*(ppm)*	*(kg/s)*	*(°C)*	*(bar)*	*(KJ/Kg)*	*(KJ/Kg - K)*	*(kW)*
1a	sea water	liquid	42000	124.4	20	2	84.02	0.296	12.46
1b	sea water	liquid	42000	124.4	35	2	146.8	0.505	209.4
2	sea water	liquid	42000	26.12	35	2	146.8	0.505	43.98
3	sea water	liquid	42000	98.24	35	2	146.8	0.505	165.4
4	sea water	liquid	42000	26.12	110	2	461.4	1.419	1269
5	sea water	vapor	--	3.19	40	0.07	2573	8.255	502.4
6	Distillate	liquid	0	3.19	30	0.07	127.5	0.442	2.191
7	sea water	liquid	47844	22.93	40	0.07	167.5	0.572	61.42
G1	geothermal	two phase	--	25.83	207	18	1200	2.398	12921
G2	geothermal	steam	--	4.26	207	18	2796	6.378	3964
G3	geothermal	liquid	--	21.57	207	18	884.7	2.398	3989
G4	geothermal	liquid	--	21.57	120	18	503.8	1.528	1273
G5	geothermal	steam	--	4.26	46	0.1	2136	6.744	693.1
G6	geothermal	liquid	--	4.26	46	0.1	191.8	0.649	18.98
G7	sea water	liquid	42000	95.1	20	2	83.93	0.296	284.9
G8	sea water	liquid	42000	95.1	41	2	171	0.583	1557
GR	geothermal	liquid	--	25.83	110	18	503.8	1.528	1273

The summary of the exergy analysis for the combined system (geothermal single flash cycle with single stage flash desalination) is presented in Table 2. The results show that the total available exergy in the two phase geothermal fluid produced by the well was 12921 kW. Of this available exergy, 3989 kW existed in the geothermal brine which was available for the desalination cycle; 1269 kW exergy was transferred to the seawater which exited the system through cooling water, reject brine and distillate product; 3964 kW was contained in the steam and connected to the single flash cycle.

TABLE 2: Summary of the exergy analysis for the combined system

Component	**Exergy Input**	**Exergy Output**	**Exergy Destroyed**	**Waste Exergy**	**Exergetic Efficiency**
	(kW)	*(kW)*	*(kW)*	*(kW)*	*(%)*
Geothermal Single Flash Cycle					
Wellhead & separator	12921	3964	4968	3989	31
Turbine	3964	2814	456	694	22
Condenser	693	19	427	247	42
Desalination Single Stage Flash Cycle					
Brine heater	5258	3706	1491	61	45
Preheater/Condenser	705	403	302	0	39
Overall combined cycle	12921	2814	7644	1002	22

As a result of irreversibilities in the system, exergy destruction occurred in all the heat exchangers of the desalination process. The exergy destruction in the combined system was found to be 7644 kW.

The low exergy efficiency in the turbine indicates that most of the exergy was transferred into the desalination cycle through the geothermal brine. The greatest exergy losses occurred in the condenser where part of the exergy was rejected through the cooling water, and the rest was reinjected in the reservoir. The exergy content of the geothermal brine still has potential to perform usable work. The work output developed by the turbine was 2814 kW, at an exergetic efficiency of 22%.

The desired exergy output from combined system in form of electricity was 2814 kW. 1557 kW of the exergy in the form of brine was discarded as waste heat. The large difference in the efficiencies shows that most of the energy received from the well, exits the plant while still containing substantial exergy.

6. TRIPLE BOTTOM LINE ASSESSMENT

The Triple Bottom-Line (TBL) is an accounting framework that incorporates three dimensions of performance: social, environmental and financial (Slaper and Hall, 2011). The purpose of including a TBL in this report is to provide a general estimation of the positive and negative impacts that might arise from the implementation of a RE-driven desalination plant in the Galápagos Islands.

Nine variables were selected based on the parameters that directly affect social, environmental and economic development in the Galápagos. Three levels of impacts were estimated according to their influence on the selected variables. Table 3 shows the variables associated with the three dimensions of performance and their estimated impacts.

TABLE 3: Triple Bottom-Line assessment of a RE-driven desalination project

#	Measures	Cost Unit	Economic		Social		Environmental	
			Positive	Negative	Positive	Negative	Positive	Negative
1	Change in land use (for irrigation)	$/m2	•••	-	••	-	-	•
2	Health-adjusted life expectancy		•	-	•••	-	-	-
3	Resource access and managment	$/m3	••	-	••	-	•••	-
4	Water Quality improvement	$/m3	•••	-	•••	-	••	-
5	Fossil fuel consumption (petrol)	$/gal	•	-	•	-	•	-
6	Electricity consumption	$/kW-h	•	-	•	-	•	-
7	Revenue by sector (contributing to GDP)	$	••	-	•	-	-	-
8	Cost of desalted water	$/m3	-	•	••	-	-	-
9	Renewable energy use	$/kW-h	••	•	••	-	•••	-

Overall, the potential benefits that a RE-driven desalination project could have in the island in terms of economic, social and environmental performance can be expected in the improvement of resource access and management, and in water quality (Table 3). The provision of fresh water through desalination will undoubtedly allow the development of goods and services that are presently conditioned by water restrictions in the island. It will also redirect the use of brackish water from the municipal tap water system so that it can be used for other economic activities such as agriculture. The lack of water for land irrigation has hampered the development of this sector, which has resulted in food imports from the mainland to sustain local demand (Palacios, 2012). This not only increases the risk of invasive species and plagues being introduced in the local ecosystem, but also prevents the sustainable development of local producers, who cannot compete with the food supply from the mainland.

The decrease in brackish water usage from aquifers will enable the natural recharge of the hydrological cycle, making the management of watersheds more sustainable. Also, the reduction of imported bottled water from mainland will reduce the amount of waste generated from plastic bottles.

Fossil fuel consumption by the water tankers that distribute the product, and the electricity consumption, presently needed to operate the water reservoirs in households, would be unnecessary under a more efficient scheme that guarantees a continuous supply of fresh water through improvements in the existing distribution system.

7. CONCLUSIONS AND RECOMMENDATIONS

7.1 Access to fresh water sources

The lack of public potable water services is clearly an ongoing problem in the Galápagos. It poses a risk to the inhabitant's health, and greatly limits the development of economic and agricultural activities linked to the use of the resource. As a result, access to potable water in Galápagos has been taken over by private businesses that operate under weak regulations regarding sanitation protocols, and a lack of permanent inspections (Liu, 2011). The need for a permanent long term solution that provides sufficient potable water, in balance with the fragile ecosystem of the islands, will rely on the innovative use of the natural resources available on site. Moreover, it will allow the local government to regain its responsibility over the provision of public services for its citizens in regards of potable water access, as stated in article 137 of the Ecuadorian Constitution (Asamblea Nacional del Ecuador, 2015).

7.2 Geothermal resources in Isabela Island

An analysis of the available information on Alcedo, Sierra Niegra and Cerro Azul was undertaken via literature reviews. Alcedo presents the most active hydrothermal system with a liquid-dominated reservoir (97% water and 3% non-condensable gases) containing neutral-chloride rich fluids. Geothermometry indicates a meteoric origin and low acidic properties of the fluid. Its proximity to the closest sea shore and its relative low volcanic activity when compared to Sierra Negra and Cerro Azul, can be seen as favourable conditions for further assessment as a potential resource. Therefore, under a preliminary broad context, the characteristics of this high enthalpy resource denote its apparent suitability to be utilized as a main heat input in a desalination process.

Additional variables in terms of location, distance to the closest town, eruptive periods, and environmental factors, will need to be considered for future development and direct use application. Further research is needed to validate the conceptual model and track possible changes in terms of geological and geochemical properties. Suggested studies include a detailed geophysics campaign with AC resistivity methods (TEM, MT, and AMT), a temperature gradient well, and an exploratory drilling campaign to obtain more information on the cap rock, host rock, and hydrothermal alteration.

7.3 Geothermal desalination project costs

A summary of the estimated upfront cost for a geothermal desalination project, including geophysical and exploratory drilling phases is presented in Table 4. The values shown are only indicative of the investment and will vary depending on the availability of the equipment and access to the location.

Desalination based on thermal separation methods is relatively simple, as the process is driven by temperature difference and its thermodynamic states, and no mechanical or moving parts are involved.

Consequently, a great percentage of the operating costs of this technique is not due to the process itself but the energy source. Fossil fuels such as coal or natural gas, are commonly use to heat the seawater for the distillation process. Operating costs can be greatly minimized when renewable energy sources such as geothermal energy is coupled with the desalination process.

The MSF-M is the industry standard and it is more suitable for large scale production ($\geq$ 100.000 m^3/day) in terms of economies of scale, but because the demand for Isabela is under 300 m^3/day and, even considering the total demand of water for the archipelago (4.500 m^3/day), the final cost of the distillate product under this configuration will not be competitive compared to other technologies. Nevertheless, the SSF-G configuration analysed in this report could produce 276 m^3/day of de-salted water from the sea, at a reasonable cost, due to its simpler design.

TABLE 4: Estimated investment costs for the proposed system (adapted from Jónsson, 2015)

Project Investment Cost		
Type	Unit	Total
Exploration cost:		
Surveys (TEM, MT, and AMT)	USD	$650 000
Total	USD	**$650 000**
Confirmation and drilling cost		
Drilling	USD	$6 000 000
Other cost	USD/Project	$20 000
Well test	USD/Well	$140 000
Well test	USD/Field	$100 000
Subtotal	USD	$6 260 000
Administration	USD/Project	$469 500
Compliance reports	USD/Project	$626 000.00
Total	USD	**$7 355 500**
Power Plant and Separators		
Separators	USD/kW	$14 000
Steam turbine	USD/kW	$1 736 000
Condenser	USD/kW	$120 400
Pump/compressor	USD/kW	$14 000
Cooling system	USD/kW	$84 000
Total	USD/kW	**$1 968 400**
Operational and maintenance cost	USD	$199 478.00
Total		**$199 478**
Capital Costs	USD	**$9 973 900**

7.4 Potabilization of distillate water

The distillate product obtained from the SSF-G is of high purity with a very small amount of dissolved salts and minerals. These properties make the water unsuitable for human consumption. Therefore, a potabilization process is required before it can be injected into the pipe distribution network for the inhabitants of Isabela. Typical treatment methods used involve carbon dioxide and hydrated lime injections, and passing carbonated water through limestone bed filters (Khawaji et al., 2008). Interestingly, as a source of carbon dioxide, CO_2 gas can be extracted from non-condensable gases in the geothermal steam and the SSF desalination vent, to be used in either potabilization methods.

7.5 Thermodynamic modelling and exergy analysis

The results from a thermodynamic model and exergy analysis of the system, using Engineering Equation Solver (EES) software, show that the geothermal resource can be successfully coupled to this desalination method. They also reveal that more work can be extracted from the exergy contained in the geothermal brine, meaning that additional low enthalpy uses might increase the project attractiveness. This exergy in the reject brine with a temperature of 40°C can be recirculated in the system, increasing the overall performance ratio of the desalination process.

7.6 Triple Bottom Line assessment

Overall, the TBL assessment denoted that potential savings on its three dimensions of performance can be achieved from the implementation of a renewable energy desalination project. Having a good quality product will reduce the government´s expenditure in treating diseases in public hospitals, which are related to water contamination cases. Consequently, it will generate a positive impact, both in the economic and social aspect.

Although it is the best alternative when compared to traditional desalination processes that use fossil fuels as the energy source, an environmental impact assessment study of the project is needed to assess possible effects that a renewable energy driven desalination system might have on the ecosystem in the Galápagos. Special attention must be placed in controlling the release of brine back into the sea, as well as road construction, CO_2 emissions, noise and disturbances to wildlife and fauna.

ACKNOWLEDGEMENTS

I gratefully acknowledge the support from Páll Valdimarsson, María Gudjónsdóttir, and Málfrídur Ómarsdóttir for their supervision and feedback. I also thank Vijay Chauhan, Lúdvík S. Georgsson and UNU-GTP staff for their support and assistance. This report is dedicated to the memory of Jerko M. Labus.

REFERENCES

Asamblea Nacional del Ecuador, 2015: *Constitución 2008. Dejemos el pasado atrás* (in Spanish). Asamblea Nacional del Ecuador – Ecuadorian Parliament, Quito, Ecuador, 223 pp.

CEPROEC-IAEN and SENPLADES, 2014: *Diagnosis and biophysical analysis for evaluation and formulation of development scenarios in the Galapagos Archipelago* (*Diagnóstico y análisis biofísico para evaluación y formulación de escenarios de desarrollo en el Archipiélago de Galápagos)*. Centro de Prospectiva Estratégica – Instituto de Altos Estudios Nacionales (CEPROEC-IAEN), Quito, Ecuador, 402 pp.

Colony, W.E., and Nordlie, B.E., 1973: Liquid sulfur at Volcano Azufre, Galapagos Islands. *Economic Geology, 68*, 371-380.

Delaney, J.R., Colony, W.E., Gerlach, T.M., and Nordlie, B.E., 1973: Geology of the Volcan Chico area on Sierra Negra volcano, Galapagos Islands. *Geological Society of America Bulletin, 84*, 2455-2470.

Dincer, I., and Rosen, M.A., 2007: *Exergy, energy, environment and sustainable development*. Elsevier, 472 pp.

DiPippo, R., and Marcille, D.F., 1984: Exergy analysis of geothermal power plants. *Geothermal Resources Council Transactions, 8*, 47–52.

DiPippo, R., 2004: Second law assessment of binary plants generating power from low-temperature geothermal fluids. *Geothermics, 33*, 565-586.

El-Dessouky, H.T., and Eltouney, H.M., 2002: *Fundamentals of salt water desalination.* Elsevier Science, Amsterdam, Netherlands, 691 pp.

Geist, D.J., 1992: An assessment of melting processes and the Galapagos hotspot: major and trace element evidence. *Journal of Volcanology and Geothermal Research, 52*, 65-82.

Geist, D.J., Howard, K.A., Jellinek, A.M., and Rayder, S., 1994: The eruptive history of Volcan Alcedo, Galapagos Archipelago: A case study of rhyolitic oceanic volcanism. *Bulletin of Volcanology, 56*, 243-260.

Geist, D.J, Howard, K.A., Larson, P., 1995: The generation of oceanic rhyolites by crystal fractionation: the basalt-rhyolite association at Volcan Alcedo, Galapagos archipelago. *Journal of Petrology, 36*, 965-982.

Geist, D.J., Naumann, T.R., and Larson, P.L., 1998: Evolution of Galápagos magmas: mantle and crustal fractionation without assimilation. *Journal of Petrology, 39*, 953–971.

Goff, F., McMurtry, G.M., Counce, D., Stimac, J., Roldan, A., and Hilton, D., 2000: Contrasting hydrothermal activity at Sierra Negra and Alcedo volcanoes, Galapagos Archipelago, Ecuador. *Bulletin of Volcanology, 62*, 34-52.

Goosen, M.F.A., Mahmoudi, H., and Ghaffour N., 2014: Today's and future challenges in applications of renewable energy technologies for desalination. *Critical Reviews in Environmental Science and Technology. 44*, 929-999.

Guyot-Téphany, J., and Liu, J., 2011: *Hydro resources in the Galápagos Islands (Recursos hídricos en las islas Galápagos).* Charles Darwin Foundation, 32 pp.

Guyot-Téphany, J., Grenier, C., and Orellana, D., 2012: *Scientific Report on survey campaign "Perceptions, use and management of water in the Galapagos"* (*Informe científico de la campaña de encuesta "Percepciones, usos y manejo del agua en Galápagos")*. Charles Darwin Foundation / University of Nantes, 86 pp.

Guyot-Téphany, J., Grenier, C., and Orellana, D., 2013: Uses, perceptions and management of water in Galapagos. In: GNPS, GCREG, CDF, and GC, *Galapagos report 2011-2012*. Galapagos National Park Service, Governing Council of Galapagos, Charles Darwin Foundation, and Galapagos Conservancy, 67-75 pp.

Ghaffour, N., Bundschuh, J., Mahmoudi, H., and Goosen, M.F.A., 2015: Renewable energy-driven desalination technologies: A comprehensive review on challenges and potential applications of integrated systems. *Desalination, 356*, 94-114.

Graham, D.W., Christie, D.M., Harpp, K.S., and Lupton, J.E., 1993: Mantle plume helium in submarine basalts from the Galapagos platform. *Science, 262*, 2023-2026.

Hey, R., 1977: Tectonic evolution of the Cocos–Nazca spreading center. *Geological Society of America Bulletin, 88*, 1401–1406.

IGEPN, 2015: Islas Galápagos. Institute of Geophysics, Polytechnic National School (IGEPN). Website: *http://www.igepn.edu.ec/islas-galapagos*

INEC, 2015: Población y demografía. National Institute of Statistics and Census. Website: *http://www.ecuadorencifras.gob.ec/censo-de-poblacion-y-vivienda/*

Jónsson, M. Th., 2015: *Mechanical design of geothermal power plants - feasibility study cost analysis, economic decision rules, NPV*. UNU-GTP, Iceland, unpublished lecture slides.

Kanoglu, M., 2002: Exergy analysis of a dual-level binary geothermal power plant. *Geothermics, 31*, 709-724.

Karytsas, C., Mendrinos, D., and Radoglou, G., 2004: The current geothermal exploration and development of the geothermal field of Milos Island in Greece. *GHC Quart. Bull., 25-2*, 17-21.

Khawaji, A.D., Kutubkhanah, I.K., and Wie, J., 2008: Advances in seawater desalination technologies. *Desalination, 221*, 47-69.

Kotas, T.J., 1985: *The exergy method of thermal plant analysis*. Butterworhts. London, Great Britain, 293 pp.

McBirney, A.R., and Williams, H., 1969: *Geology and petrology of the Galapagos Islands*. Geological Society of America, Memoir 118, 197 pp.

MEER, 2015: Zero Fossil fuels in Galapagos (Cero combustibles fósiles en Galápagos). Ministry of Electricity and Renewable Energy (MEER). Website: http://www.energia.gob.ec/cero-combustibles-fosiles-en-galapagos-2/

Naumann, T., and Geist, D.J., 2000: Physical volcanology and structural development of Cerro Azul volcano, Isabela Island, Galápagos: Implications for the development of Galapagos-type shield volcanoes. *Bulletin of Volcanology, 61*, 497-514.

Naumann, T., Geist, D.J., and Kurz, M., 2002: Petrology and geochemistry of Volcan Cerro Azul: Petrologic diversity among the western Galapagos volcanoes. *Journal of Petrology, 43*, 859-883.

Neall, V.E., and Trewick, S.A, 2008: The age and origin of the Pacific islands: A geological overview. *Philosophical Transactions of the Royal Society of London B: Biological Sciences, 363*, 3293–3308.

Liu, J., 2011: *Investigation of the microbiological quality of water and water-related diseases in the island Santa Cruz*. (*Investigación de la calidad microbiológica del agua y de las enfermedades relacionadas al agua en la isla Santa Cruz)*. Charles Darwin Foundation, unpublished report, 67 pp.

Living Galápagos, 2015: Dirty water 2013. Website: http://livinggalapagos.org/en/dirty-water/

López, J., Rueda, D., and Nakaya, S., 2007: Water quality monitoring on Isabela Island - annual report. (Monitoreo de calidad del agua en la isla Isabela - Informe annual). Dirección Nacional Parque Galápagos (DNPG) and Japan International Cooperation Agency (JICA), Puerto Ayora, Galapagos, Ecuador, 29 pp.

Olsson, G., 2015: *Water and energy: Threats and opportunities* (2nd ed.). IWA Publishing, London, United Kingdom, 496 pp.

Palacios, P., 2012: *Conceptual analysis of local food chains in the market. Local chains Galapagos Project, Product V. (Análisis conceptual de los encadenamientos locales en el mercado alimenticio. Proyecto Encadenamientos Locales Galápagos, Producto V).* Charles Darwin Foundation, 1-7.

Simkin, T., 1984: Geology of Galapagos. *Biological Journal of the Linnean Society, 21*, 61-75.

Schilling, J.G., Anderson, R.N., and Vogt, P., 1976: Rare earth Fe and Ti variations along the Galápagos spreading centre, and their relationship to the Galápagos mantle plume. *Nature, 261*, 108–113.

Slaper, T.F., and Hall, T.J., 2011: The triple bottom line: What is it and how does it work? *Indiana Business Review, 86*, 4-8.

Verma, S.P., Schilling, J.G., and Waggoner, D.G., 1983. Neodymium isotopic evidence for Galápagos hotspot-spreading center system evolution. *Nature, 306*, 654–657.

Walsh, J., McCleary A., Heumann, B., 2010: Community expansion and infrastructure development: implications for human health and environmental quality in the Galapagos Islands of Ecuador. *Journal of Latin American Geography, 9*, 137-159.

Wark, K.J., 1995: *Advanced Thermodynamics for Engineers*. McGraw-Hill, New York, United States, 326 pp.

White, W.M., McBirney, A.R., and Duncan, R.A., 1993: Petrology and geochemistry of the Galapagos Islands: portrait of a pathological mantle plume. *Journal of Geophysical Research, 98*, 533-563.

WHO, 2003: *Sodium in drinking-water. Background document for development of WHO guidelines for drinking-water quality*. World Health Organization (WHO), Geneva, Switzerland, document WHO/SDE/WSH/03.04/15, 11 pp.